

AFFDL-TR-71-155

Part I

~~SECRET~~
~~CONFIDENTIAL~~
~~CONFIDENTIAL~~

**TAKEOFF AND LANDING ANALYSIS (TOLA)
COMPUTER PROGRAM**

Part I. Capabilities of the Takeoff and Landing Analysis Computer Program

URBAN H. D. LYNCH, CAPTAIN, USAF

Approved for public release; distribution unlimited.

FOREWORD

This report was prepared by personnel of the Flight Mechanics Division of the Air Force Flight Dynamics Laboratory and the Digital Computation Division of the Aeronautical Systems Division. The report was prepared under Project 1431, "Flight Path Analysis," Task 143109. "Trajectory and Motion Analysis of Flight Vehicles." The formulation and interim documentation were completed by Capt. Urban H.D. Lynch. Programming was accomplished by Mr. Fay O. Young of the Digital Computation Division (ASVCP), Computer Science Center, Aeronautical Systems Division.

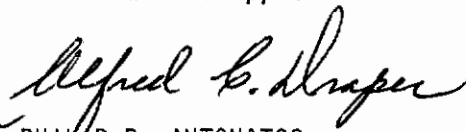
This report is prepared by Capt Lynch and Mr. John J. Dueweke of the High Speed Aero Performance Branch (FXG), and combines the applicable portions of FDL-TDR-64-1, Part 1, Volume 1, with the interim documentation prepared by Capt. Lynch.

This report is divided into four parts:

- Part I: Capabilities of the Takeoff and Landing Analysis Computer Program
- Part II: Problem Formulation
- Part III: User's Manual
- Part IV: Programmer's Manual

This report was submitted by the author in November 1971.

This technical report has been reviewed and is approved.


for PHILIP P. ANTONATOS
Chief, Flight Mechanics Division
Air Force Flight Dynamics Lab.

ABSTRACT

TOLA is an acronym for a takeoff and landing analysis digital computer program. This part of the report discusses capabilities of the TOLA program.

The program provides a complete simulation of the aircraft takeoff and landing problem. Effects simulated in the program include: (1) aircraft control and performance during glide slope, flare, landing roll, and takeoff roll, all under conditions of changing winds, engine failures, brake failures, control system failures, strut failures, runway length and control variable limits, and time lags; (2) landing gear loads and dynamics for aircraft with up to five gears; (3) multiple engine aircraft; (4) engine reversing; (5) drag chute and spoiler effects; (6) braking; (7) aerodynamic ground effect; (8) takeoff from aircraft carriers; and (9) inclined runways and runway perturbations. The program is modular so that glide slope, flare, landing, and takeoff can be studied separately or in combination.

Results from this computer program compared well with those of other programs and actual test results. The program is very versatile through its completeness in the simulation of the many systems and effects involved in the takeoff and landing problem. Application of TOLA has shown the need for a total system analysis since many unexpected results have been obtained.

Contrails

AFFDL-TR-71-155
Part I

The TOLA program is ideal for dynamic tradeoff studies in aircraft design, landing gear design and landing techniques. The formulation is programmed for both the IBM 7094/7044 II Direct Couple Computer System in the FORTRAN IV Computer Language and the CDC 6400/6500/6600 Scope 3.3 Computer System in the FORTRAN EXTENDED Computer Language.

Contrails

AFFDL-TR-71-155

Part I

TABLE OF CONTENTS

SECTION	PAGE
I INTRODUCTION	1
II PROBLEM ANALYSIS	3
1. Definition	3
2. Equations of Motion	3
3. Landing Gear	4
4. Autopilot	5
5. Computer Output	12
III ANALYTICAL RESULTS	14
1. Glide Slope	14
2. Flare	17
3. Landing Roll	20
4. Takeoff Roll	27
IV CONCLUSIONS	29

ILLUSTRATIONS

FIGURE	PAGE
1. C-5A Strut Configuration	5
2. Aircraft Autopilot	6
3. Autopilot Control Systems	7
4. Pitch Autopilot Schematic	11
5. Nominal Glide Slope	15
6. Glide Slope with Headwind Change	16
7. Crossrange Control with Sidewind Change and Engine 1 Failure	16
8. Nominal Flare	18
9. Long Flare	19
10. Short Flare Crabbed	21
11. Ground Reaction Pitch Moment	30
12. Pitch Rate	30
13. Pitch Angle	30
14. Normal Axis Ground Reaction	30
15. Normal Axis Acceleration	30
16. Mass Center Sink Rate	30
17. Mass Center Altitude	30
18. Longitudinal Axis Acceleration	30
19. Runway Velocity	31
20. Tire Deflection, Gear 5	31
21. Ground Force, Gear 5	31
22. Strut Velocity, Gear 5	31
23. Strut Displacement, Gear 5	31

ILLUSTRATION (Cont)

FIGURE	PAGE
24. Wheel Axle Moment, Gear 5	31
25. Tire Angular Rate, Gear 5	31
26. Tire Deflection, Gear 3	31
27. Ground Force, Gear 3	32
28. Strut Velocity, Gear 3	32
29. Strut Displacement, Gear 3	32
30. Wheel Axle Moment, Gear 3	32
31. Tire Angular Rate, Gear 3	32
32. Tire Deflection, Gear 1	32
33. Ground Force, Gear 1	32
34. Strut Resistance, Gear 1	32
35. Upper Air Chamber Pressure, Gear 1	33
36. Strut Acceleration, Gear 1	33
37. Strut Velocity, Gear 1	33
38. Strut Displacement, Gear 1	33
39. Lower Air Chamber Pressure, Gear 1	33
40. Secondary Piston Acceleration, Gear 1	33
41. Secondary Piston Velocity, Gear 1	33
42. Secondary Piston Displacement, Gear 1	33
43. Wheel Axle Moment, Gear 1	34
44. Tire Angular Rate, Gear 1	34
45. Ground Reaction Pitch Moment	34
46. Pitch Rate	34
47. Pitch Angle	34

ILLUSTRATIONS (Cont)

FIGURE	PAGE
48. Normal Axis Ground Reaction	34
49. Mass Center Sink Rate	34
50. Mass Center Altitude	34
51. Runway Velocity	35
52. Tire Deflection, Gear 1	35
53. Ground Force, Gear 1	35
54. Strut Displacement, Gear 1	35
55. Tire Deflection, Gear 3	35
56. Ground Force, Gear 3	35
57. Strut Displacement, Gear 3	35
58. Tire Deflection, Gear 5	35
59. Ground Force, Gear 5	36
60. Strut Displacement, Gear 5	36

NOMENCLATURE

\bar{F}_T	total vector force acting on aircraft
M_T	total mass of aircraft
$\ddot{\bar{R}}$	inertial vector acceleration of nominal mass center
K	number of gears
m_k	mass of moving part of k^{th} gear
$(\ddot{\bar{r}}_{kc})_k$	vector acceleration of mass center of m_k relative to aircraft
\bar{M}_O	total vector moment acting on aircraft about nominal mass center
\bar{I}_O	aircraft moment of inertia tensor about nominal mass center
$\dot{\bar{\omega}}_O$	inertial angular acceleration vector
$\bar{\omega}_O$	inertial rotation rate vector
$(\bar{R}_k)_O$	vector from nominal mass center to the wing-gear root of k^{th} gear
\bar{r}_{kc}	vector from wing-gear root to mass center of m_k
α_d	desired angle of attack
δ_{qn}	nominal elevator trim position
α	actual angle of attack
$\dot{\alpha}$	$d\alpha/dt$
$\dot{\alpha}_d$	$d\alpha_d/dt$
R_{fa}	rate feedback constant
Δa	allowed angle of attack error
δ_{qd}	desired elevator position
P_h	elevator deflection/error constant

Contrails

SECTION I
INTRODUCTION

The design of an aircraft requires that the landing gear system be designed to interface properly with the airframe and to be compatible with other systems affecting takeoff and landing performance. Of these systems, the primary ones are the landing gear system, the power system, the elevator control system, and the rudder control system. Usually, the landing gear design is based primarily on vehicle initial impact; the power system requirement is based primarily on climb or cruise performance; elevator size is based primarily on vehicle rotation at liftoff airspeed; and rudder size is based primarily on engine out conditions. The final evaluation of all these systems during takeoff and landing, however, lies in the answer to the question: How do all the systems perform as a unit? The TOLA (takeoff and landing analysis) computer program attempts to generalize the aircraft, the capability of the main aircraft control systems, and the landing-takeoff situation into a single comprehensive calculation to answer this question. The program does not perform the design function; it simply takes input data on the systems and computes dynamic results.

The program is very versatile through its completeness in the simulation of the many systems and effects involved in the takeoff and landing problem. The following list of complex problems are within TOLA's capability and are suggestive of its completeness:

- a. What effect does limited runway length, changing winds, and engine failure have on a go-around decision for a particular situation?

AFFDL-TR-71-155

Part I

b. How does a change in the control schedule for the landing roll affect maximum gear loads? (Spoiler activation and not initial impact appears to play a significant roll here.)

c. What limitations would have to be placed on the landing if one strut failed to brake or to extend from the fuselage?

d. With multiple engine aircraft and a thrust reversing capability, is it safe to have some engines in reverse during landing in view of possible engine failure?

e. How nonsymmetrical can the landing impact be and yet provide an acceptable landing?

This part of the report discusses the TOLA simulation and its capabilities by specific application to the Air Force C-5A aircraft.

SECTION II PROBLEM ANALYSIS

1. DEFINITION

In this report, the landing problem is broken down into four main areas: glide slope, flare, landing roll, and takeoff roll. For the glide slope, the basic requirement is to remain near the glide slope position and come down at a constant inertial speed. For the flare, the basic requirement is to touchdown at a desired sink rate and landing speed so as to meet the limitations of expected landing roll distance and remaining runway length. For the landing roll, the basic requirement, is to sequence the spoilers, engine throttle, thrust reversers, drag chute, and braking to bring the aircraft speed down to the taxi speed. For the takeoff roll, the basic requirement is to rotate the aircraft to the lift-off attitude at the proper airspeed. These requirements must be met subject to changing winds, control deflection limits and time lags, aerodynamic ground effect transition, engine failures, and selected braking failures.

2. EQUATIONS OF MOTION

The equations of motion assume that the main aircraft frame is rigid; the dynamic effects of up to five independent landing gears, however, are included in the equations. Equations 1 and 2 are the two-vector rigid-body equations of motion when moving gears are included (for details see Part II).

$$\bar{F}_T = m_T \ddot{\bar{R}} + \sum_{k=1}^K m_k (\ddot{\bar{r}}_{kc})_k \quad (1)$$

$$\bar{M}_O = \bar{I}_O \cdot \dot{\bar{\omega}}_O + \bar{\omega}_O \times (\bar{I}_O \cdot \bar{\omega}_O) + \sum_{k=1}^K m_k [(\bar{R}_k)_O + \bar{r}_{kc}] \times (\ddot{\bar{r}}_{kc})_k \quad (2)$$

3. LANDING GEAR

The landing gear model, shown in Figure 1, is a double air chamber oleo strut with balloon tires, similar to that used on the C-5A aircraft; the secondary piston and air chamber can be eliminated from the problem, if desired. Each of the struts must lie in a plane parallel to the aircraft plane of symmetry, but the strut axis may be nonperpendicular to the longitudinal aircraft axis. The position and velocity of each strut and secondary piston are obtained by numerical integration subject to position constraints (for example, the main strut must move within the limits of the fully extended position and strut bottom position). Orifice coefficients can depend on the direction of oil flow through the orifice. Wing-gear root friction (i.e., binding friction between moving strut and its support at the wing) is also included. Tire forces depend upon tire deflection and a coefficient of friction which is a function of "percent skid" (i.e., the ratio of tire footprint velocity to axle velocity). The simulation is designed to consider that the gears may bounce off and back onto the runway.

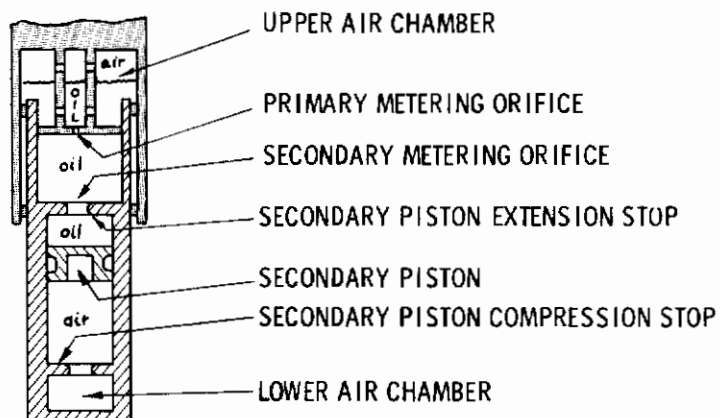


Figure 1. C-5A Strut Configuration

4. AUTOPILOT

The function of the autopilot is to specify the magnitude of the control variables (within the capability of the aircraft) that will result in aircraft performance to satisfy the basic requirements of the glide slope, flare, landing roll, and takeoff roll. As such, the autopilot performs three functions:

- (a) Senses errors;
- (b) Defines a maneuver to correct the errors; and
- (c) Specifies the magnitudes of the control variables to achieve the corrective maneuver.

Figure 2 is a basic functional diagram of the autopilot. The maneuver logic takes information on the state of the aircraft, computes errors, and defines a corrective maneuver by specifying angle of attack, angle of sideslip, roll angle, thrust, condition of engines

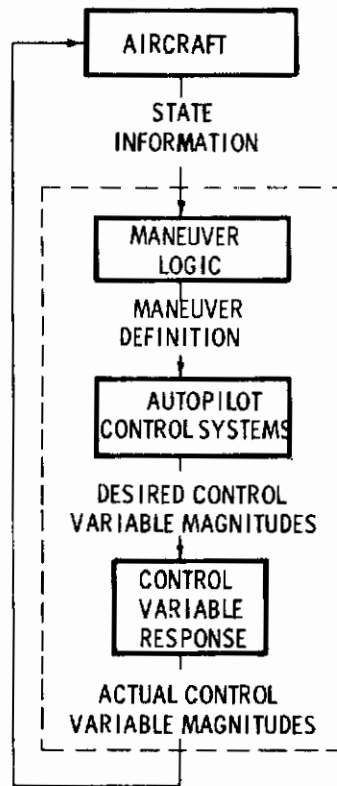


Figure 2. Aircraft Autopilot

and brakes, and the staging of events such as spoiler actuation, kill power, reversing the engines, drag chute deployment, and brake actuation. The autopilot control systems then take the output information from the maneuver logic and determines the desired magnitudes of the control variables. These values are then sent through a basic model of control variable response where control variable lags are simulated. The actual control variable magnitudes then determine aircraft response.

Figure 3 shows the maneuver logic and autopilot control system in more detail.

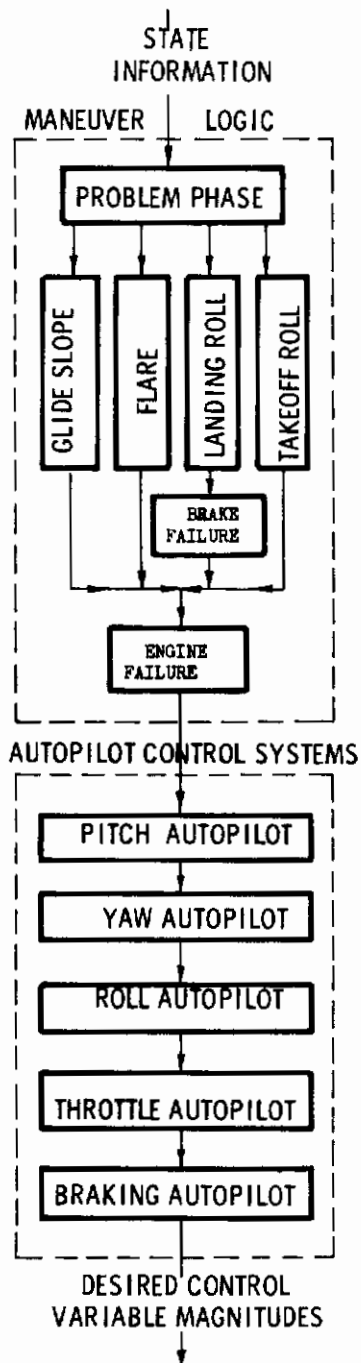


Figure 3. Autopilot Control Systems

AFFDL-TR-71-155
Part I

a. Maneuver Logic

The maneuver logic is divided into four main phases: glide slope, flare, landing roll, and takeoff roll. The glide slope phase determines the trim angle of attack and thrust needed to maintain the inertial glide slope velocity magnitude and direction. In a cross wind situation, the aircraft is "crabbed" into the wind. Long period motion in the glide slope vertical plane is damped by modifying the trim angle of attack command, and long period motion in the horizontal plane is damped by commanding slight roll angles about the level wing position.

The flare phase begins at an arbitrary altitude set during data input. The aircraft is then required to perform a constant acceleration flare that results in touchdown at a specific vector position and vector velocity, which are limited by an expected landing distance and known runway length. Because of the slight lags and overshoots in aircraft response, the possible effects of engine failures, wind changes, and limited aircraft flare capability for a given situation, the magnitude of the constant acceleration is continually updated subject to acceptable touchdown constraints. A "hold mode" is entered as the aircraft nears the ground, where all controls usually remain fixed except for a decrab in the case of a cross-wind landing, and a possible pitch maneuver to limit the maximum pitch angle near the ground. A "kill power" option is also provided in the hold mode if desired.

The landing roll phase begins as soon as any one of the gear tires touches the runway. From this point, nearly all control is determined

Contrails

AFFDL-TR-71-155
Part I

by time after impact. The following events can be staged, if desired: deploy spoilers; deploy drag chute; kill power; reverse engines; apply brakes; brake failures; and a gradual change of elevator position. Throughout the landing roll, roll control is reduced to zero and the yaw autopilot attempts to keep the aircraft's longitudinal axis parallel to the runway center line. The landing roll can be terminated on either position, velocity, or time.

The takeoff roll phase begins from a near equilibrium position for the aircraft and landing gears. Throttle position is commanded at a "takeoff" value. The elevator deflection is left at a fixed input value until a particular takeoff airspeed is obtained. At that time, a takeoff angle of attack is commanded. As with the landing roll phase, roll control is zero and the yaw autopilot attempts to keep the aircraft's longitudinal axis parallel to the runway center line. The takeoff roll phase is terminated on a preprogrammed aircraft altitude above the runway.

Prior to entering the autopilot control systems, a check on engine failures is made.

b. Autopilot Control Systems

Five major autopilot control systems are simulated: pitch, yaw, roll, throttle, and braking.

The function of the pitch autopilot is to command the elevator position to achieve the desired angle of attack received from the maneuver

AFFDL-TR-71-155

Part I

logic. Let us examine Figure 4. The pitch autopilot first evaluates the nominal elevator trim position, δ_{qn} , by evaluating the static aerodynamic pitch moments at the desired angle of attack and the engine thrust pitch moments. The angle of attack error signal, α_e , is composed of a position error and a relative rate feedback error. The amount of rate feedback error is determined by an input constant, $R_{f\alpha}$. The angle of attack error signal is allowed to have a fixed error, $\Delta\alpha$ (also set by data input). If the angle of attack error falls within the allowed fixed error, the desired elevator position, δ_{qd} , becomes the nominal trim position. If the angle of attack error is outside the allowed fixed error, the desired elevator deflection is a linear combination of the nominal trim position and a constant, P_h , times the angle of attack error. The desired elevator deflection is finally limited by the upper and lower deflection limits of the elevator. By appropriately selecting the allowed error constant, the rate feedback constant, and the constant defining the ratio between elevator deflection and angle of attack error, a pitch autopilot can be built to meet the needs of a specific aircraft configuration. The yaw and roll autopilots are similar in concept to the pitch autopilot.

The function of the throttle autopilot is to command throttle settings that result in the thrust requested by the maneuver logic. The throttle autopilot can simulate up to four independent engine locations. A throttle fix logic is provided so that any of the engines may be fixed forward or reverse. The remaining engines not in a fixed mode are variable throttle and are required to complement the fixed throttle engines in achieving the thrust requested by the maneuver logic. This

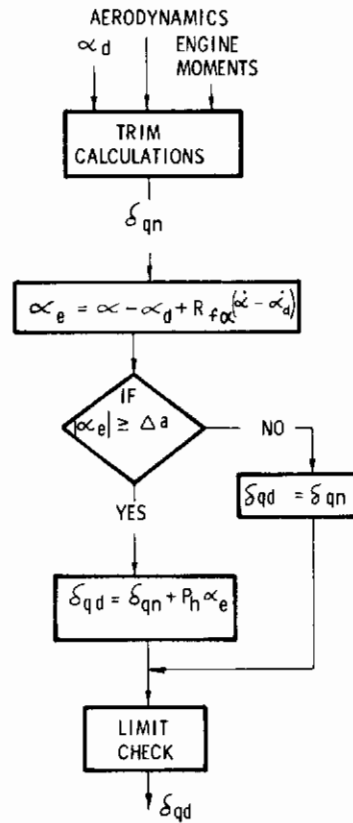


Figure 4. Pitch Autopilot Schematic

AFFDL-TR-71-155

Part I

allows landing studies to be done with some engines in reverse and others forward. In either the fixed or variable modes, almost any combination of engine failures can be staged. When an engine failure combination occurs, the remaining variable engines are required to meet the requested thrust if physically possible; they can also carry different thrust loads, if desired. When engaging reverse thrust, a throttle constraint can be applied, if desired; that is, one can require the actual throttle setting to be below a fixed value before engaging reverse. There are no constraints in going from reverse to forward thrust.

The brake autopilot controls the braking moment applied about the axle of each gear strut individually. Four options are provided for each landing gear: (1) a constant braking moment set for each gear at data input, which is similar to applying constant braking pressure; (2) a controlled braking option, in which wheel angular speed is controlled by the braking moment to keep the "percent skid" of the tires a constant; this indirectly controls the tire-runway coefficient of friction to be a constant; (3) a failure mode simulating no braking moment; and (4) a failure mode simulating a locked wheel where the tire rotational speed would be zero. The staging of braking options for each gear is done in the brake failure logic.

5. COMPUTER OUTPUT

The output information on TOLA is explained in detail in Part III of this report. The following word description of the output is

Contrails

AFFDL-TR-71-155

Part I

presented to give the potential users an idea of the kinds of information computed:

- a. Six-degree of freedom information for the general airframe.
- b. Complete information on the state of the maneuver logic, five autopilots, and control response.
- c. Complete information on the dynamic state of the five landing gears.

The next section shows some calculations done on the Air Force C-5A aircraft and presents a major portion of the output mentioned above.

SECTION III ANALYTICAL RESULTS

1. GLIDE SLOPE

Figure 5 shows the changes required in trim angle of attack, α_d , trim thrust, T_d , and trim elevator position, δ_{qn} , to maintain glide slope position and velocity as the C-5 A aircraft begins the transition into ground effect. The calculation began with the aircraft in a trimmed condition on the glide slope at 300 feet altitude. The glide slope was terminated at 100 feet altitude, where the flare began. Error in glide slope altitude was maintained to less than 0.5 ft, and in velocity down the glide slope to less than 0.5 ft/sec. (Note that the angle of attack and power required to maintain the glide slope are reduced, and that even though the pilot wants to nose the aircraft over, the required reduction in thrust and increasing effectiveness of the horizontal stabilizer dictate that he pull back on the stick.)

Figure 6 shows results for the same glide slope situation except a sudden 20 ft/sec headwind is encountered at approximately 300 ft altitude. Glide slope position and velocity are controlled very well. Phugoid damping was essential to maintain the glide slope vertical position.

Figure 7 shows the resulting cross range control for a sudden right sidewind encounter of 20 ft/sec at 300 ft altitude followed by a right outboard engine failure at 200 ft altitude. The aircraft is "crabbed" into the wind to take out the major cross range disturbing force and is rolled slightly right and then left to dampen out horizontal oscillations

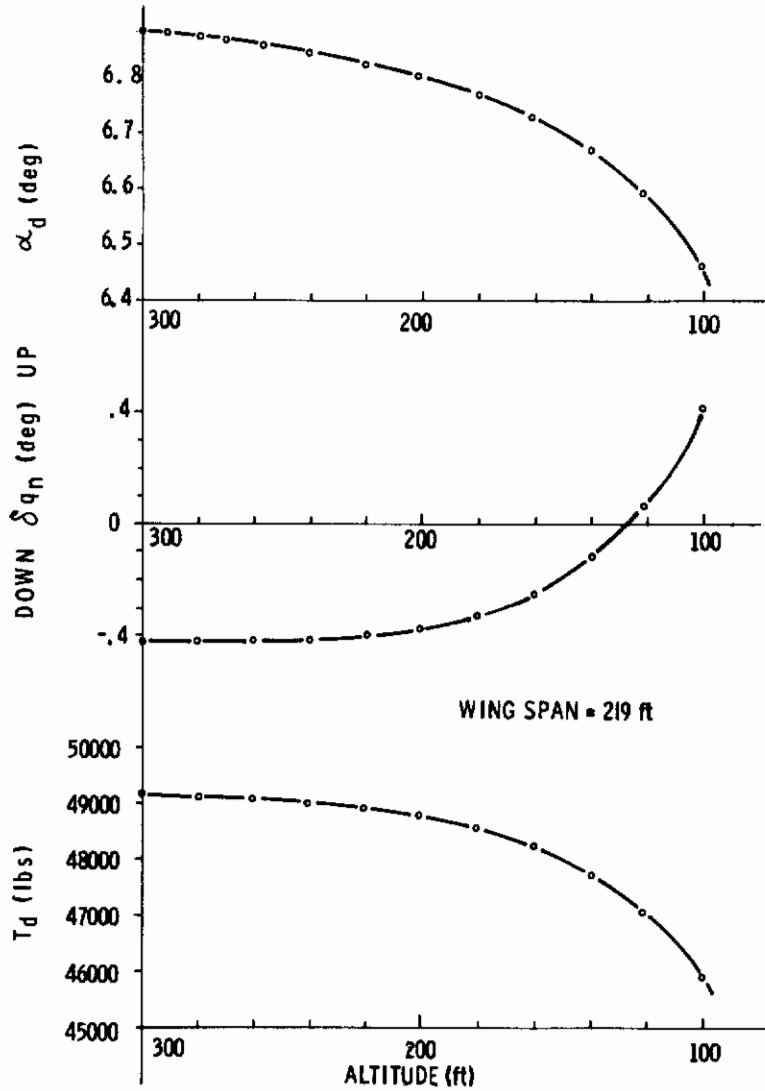


Figure 5. Nominal Glide Slope

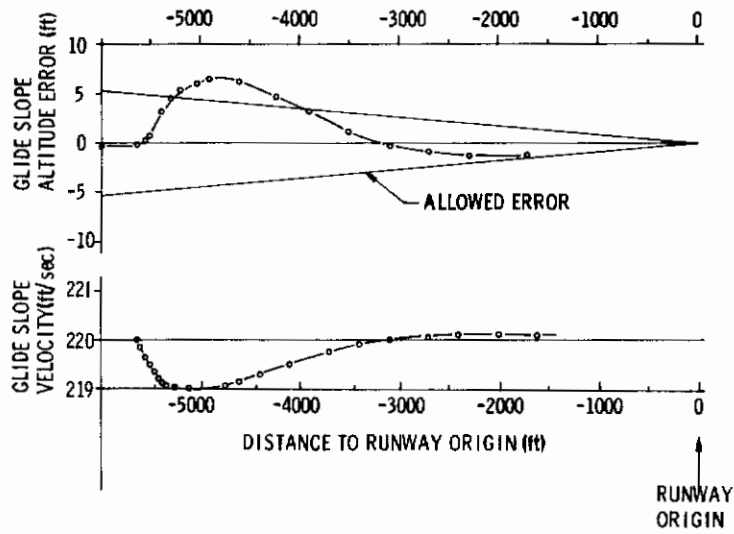


Figure 6. Glide Slope with Headwind Change

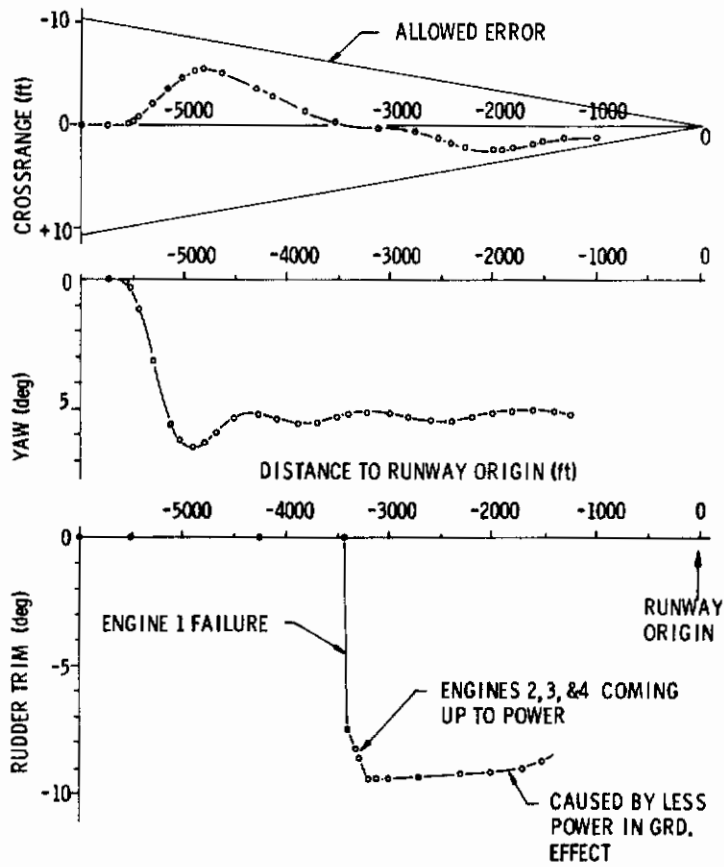


Figure 7. Crossrange Control with Sidewind Change and Engine 1 Failure

AFFDL-TR-71-155

Part I

and maintain the ground track. The yaw autopilot and throttle autopilot response to the right outboard engine failure is so quick that little noticeable perturbation in glide slope performance occurs. The lower part of Figure 7 shows the rudder trim required because of engine failure. Immediately on failure the left rudder trim required is 7.43 degrees. In this particular calculation, the remaining three working engines were requested to each carry one third of the required glide slope thrust. As the three working engines come up to power, the rudder trim gradually increases to 9.40 degrees. Because of ground effect, the required thrust in the glide slope decreases and so does the required rudder trim. Glide slope altitude error was less than 3 ft and velocity error was less than 0.5 ft/sec.

2. FLARE

Figure 8 shows nominal flare performance for a case of unlimited runway length. It was initially requested to set the aircraft down at runway position +100 ft, at a sink rate of 1 ft/sec, and a landing speed of 200 ft/sec. Since plenty of runway exists, the flare logic elects a nominal runway touchdown position of approximately +850 ft and the touchdown velocity constraints remain unchanged. Actual touchdown conditions were as follows: runway position - +890 ft; sink rate - 1.6 ft/sec; and landing speed - 197 ft/sec. Figure 8 shows the actual angle of attack, α , and desired angle of attack, α_d , sink rate, ground speed, and altitude histories.

Figure 9 shows flare performance for the same situation as Figure 8 except there is a limited runway length that forces touchdown to occur

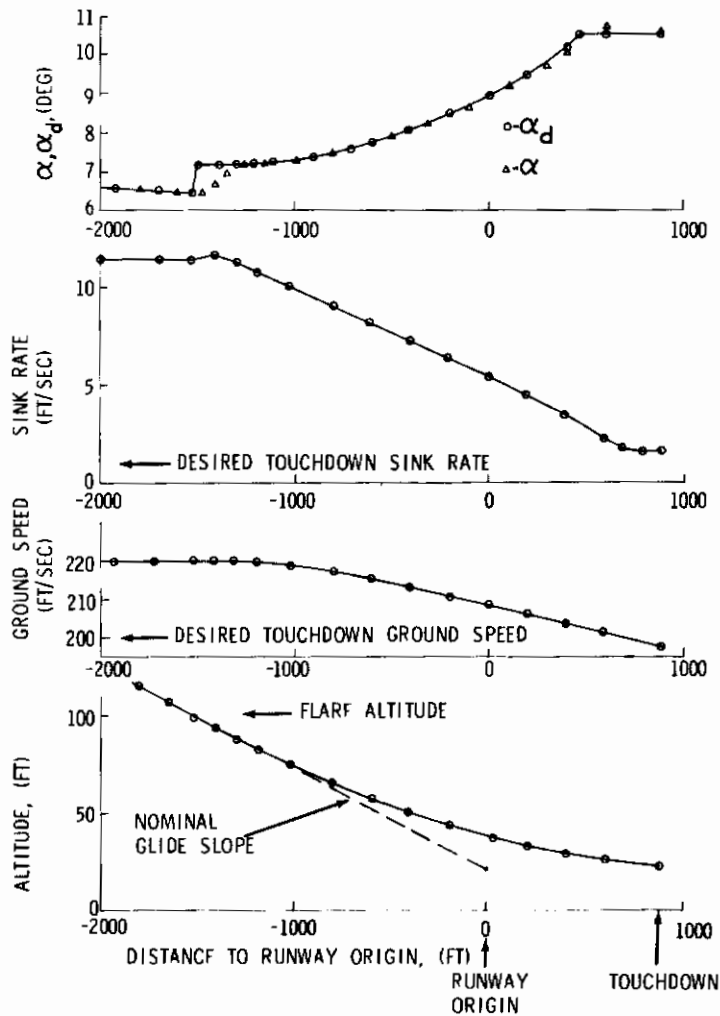


Figure 8. Nominal Flare

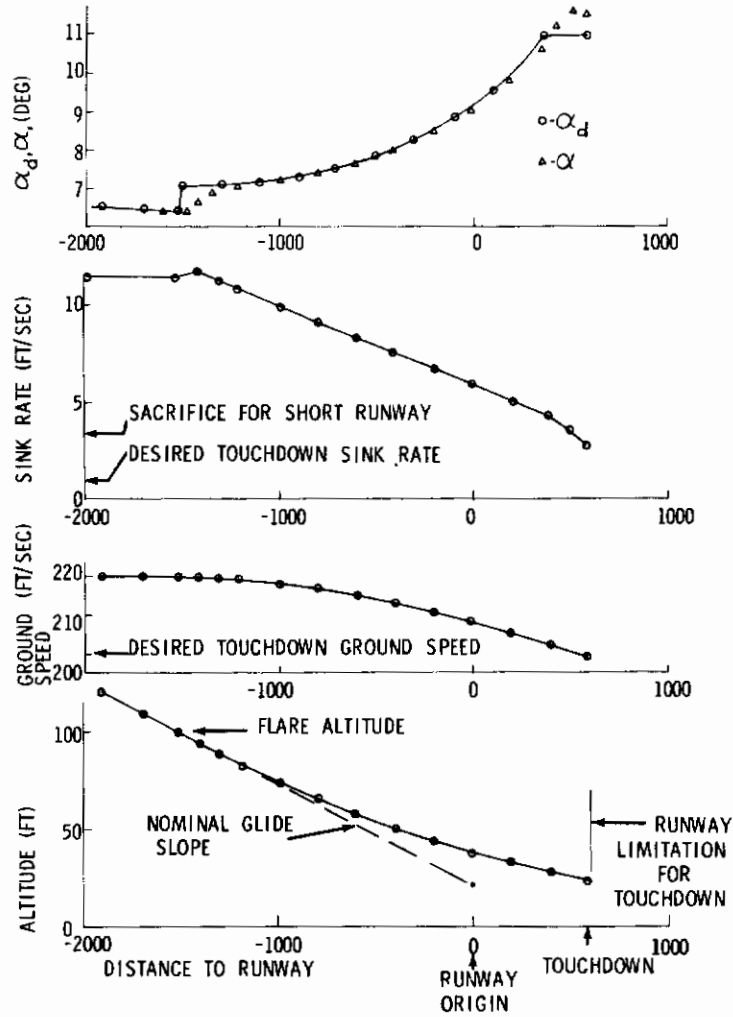


Figure 9. Long Flare

AFFDL-TR-71-155
Part I

no further than the 600 ft runway position. The flare logic senses the situation and elects to touchdown at the limiting runway position which requires a sacrifice of the desired touchdown sink rate from 1 ft/sec to 3.3 ft/sec. Desired landing speed remains unchanged. Actual touchdown conditions were as follows: runway position - 585 ft; sink rate - 2.7 ft/sec; and landing speed - 199 ft/sec. Data plotted in Figure 9 is similar to that plotted in Figure 8.

Figure 10 shows flare performance for the same situation as Figure 8 except the aircraft is crabbed into a right sidewind of 20 ft/sec and the flare is short, forcing touchdown to occur at least after the 1000 ft runway position. The decrab begins in the hold mode when the main gear wheels are approximately 7 feet above the runway. Actual touchdown conditions were as follows: sink rate - 1.48 ft/sec; runway position - 1167 ft; landing speed - 201 ft/sec; horizontal flight path angle - -0.27 degrees, and yaw-angle - -0.68 degree.

3. LANDING ROLL

To show the capability of the simulation in the landing roll, one complete landing roll calculation is shown by computer plots. The planned landing roll was as follows: landing weight - 635,850 lbs; landing speed - 200 ft/sec; sink rate - 5 ft/sec; trim angle of attack - 10 degrees; inboard engines fixed reverse - 10,000 lbs each; outboard engines forward at 30,000 lbs each (engines had to be at idle speed to actuate reverse); actuate spoilers 1 second after touchdown; begin controlled braking (coefficient of friction 0.2) at 2 seconds after touchdown; begin engine reverse at 3 seconds after touchdown; and begin elevator nose-over at 5 seconds after touchdown.

AFFDL-TR-71-155
Part I

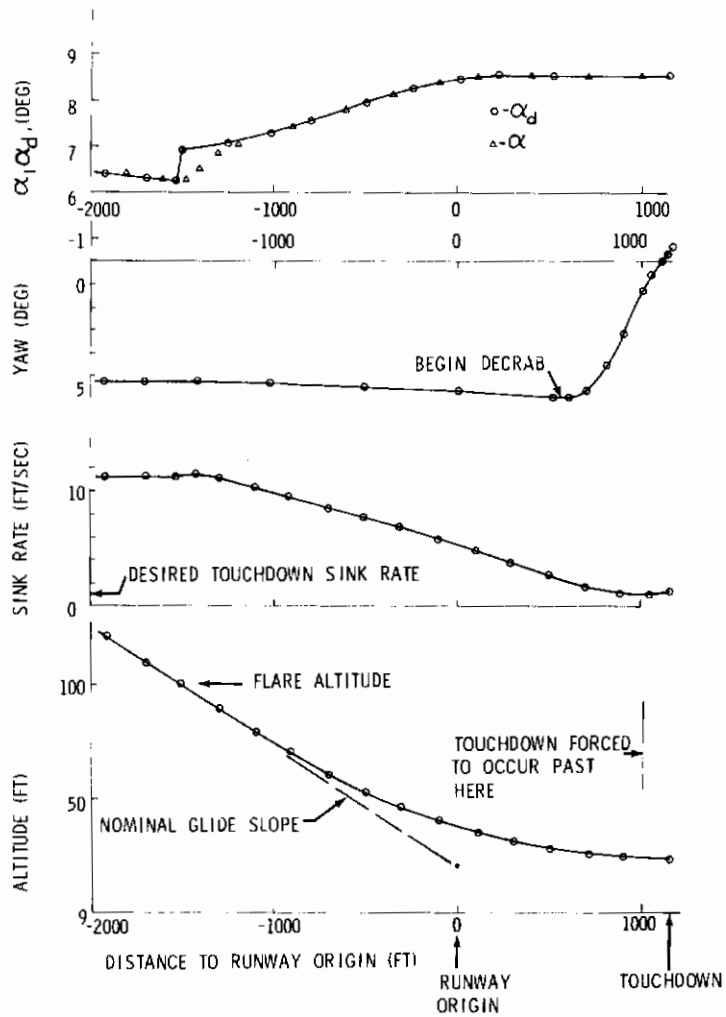


Figure 10. Short Flare Crabbed

Contrails

AFFDL-TR-71-155
Part I

Table I lists the major events throughout this particular landing roll. Strut 1 refers to the nose gear, struts 2 and 3 to the forward main gears, and struts 4 and 5 to the back main gears. Because the impact was planned symmetric, the response is essentially the same for struts 2 and 3 and for struts 4 and 5. The simulation is capable of analyzing unsymmetric impact. Figures 11 through 44 show the computer output plotted every 0.05 seconds from 0 to 23 seconds to indicate the long-term response of the aircraft. The actual integration interval -- obtained by a variable-step Runge Kutta method -- is much smaller than the plotting interval, which explains what might appear to be discontinuities in the plots.

Figures 11 thru 19 show the rigid body response of the main airframe. Figure 11 shows the total ground reaction pitch moment that is transmitted to the aircraft main frame by all five landing gears. The first negative impulse (between 0.14 and 1.14 seconds) was caused by initial impact of gears 4 and 5, which are behind the aircraft's mass center. Spoilers were actuated at 1.14 seconds, causing the aircraft to sink back onto the runway, which produced a second, much larger, negative impulse between 1.14 and 2.54 seconds. Nose gear impact at 2.54 seconds caused the pitch moment to go positive. The nose gear bounced at 3.14 seconds, and the pitch moment once again went negative. The nose gear impacted for the second and last time at 3.64 seconds, and once again the pitch moment went slightly positive. The braking which began at 2.14 seconds, kept the pitch moment negative; the pitching moment finally damps about zero as the aircraft slows to taxi speed.

TABLE I
LANDING ROLL EVENTS

Time (Sec)	Event
0.140	Initial impact of tires 4 and 5
0.160	Struts 4 and 5 move
0.760	Sink rate reduced to zero
1.06	Sink rate -1.307 ft/sec
1.140	Spoilers activated
1.690	Struts 2 and 3 impact and move and secondary pistons in 4 and 5 move
2.140	Secondary pistons in 4 and 5 back, braking
2.540	Nose strut 1 impacts and moves
2.590	Secondary piston in 1 moves
2.790	Secondary pistons in 2 and 3 move
2.890	Secondary pistons in 2 and 3 back
2.990	Secondary piston in 1 back
3.140	Landing reverse signal, nose gear 1 bounces
3.390	Nose strut 1 back
3.540	Secondary pistons in 4 and 5 move
3.640	Nose gear impact second time
3.69	Strut 1 moves, secondary pistons in 4 and 5 back
5.14	Elevator nose over begins
9.94	Inboard engines up to full reverse
9.99	Outboard engines to reverse throttle constraint
16.84	Elevator nose over complete
17.59	Outboard engines at full reverse
23.29	Calculation stopped

Contrails

AFFDL-TR-71-155
Part I

Figure 12 shows the pitch rate which begins at zero and finally damps to zero. Figure 13 shows the pitch angle which damps to a slight nose down attitude, caused mainly by the braking forces and reverse thrust. Figure 14 shows the ground reaction force transmitted to the main airframe normal to the longitudinal axis. Note that the largest load does not occur on impact or even immediately after spoiler activation, but is 1,180,000 lbs (almost twice the aircraft weight) at 2.80 seconds. The ground reaction normal force finally damps to the aircraft weight, as expected.

Figure 15 shows the total aircraft normal acceleration, which includes all forces except gravity. As expected from Figure 14, the highest g loading occurred at 2.80 seconds and damped to -32.2 ft/sec^2 . Figure 16 shows the aircraft sink rate history. Impact occurred at 5 ft/sec, as planned, went to a higher value 5.6 ft/sec after spoiler activation, and damped to zero, as expected. Figure 17 shows the aircraft altitude history, which finally damped to a stable value of 19.05 ft. Figure 18 shows the longitudinal aircraft axis acceleration achieved by controlled braking (0.2 coefficient of friction) and engine reverse. Figure 19 shows the landing speed history. The calculation was terminated at 12.80 ft/sec landing speed, at which time the aircraft had moved down the runway 2650 ft from the impact point.

Figures 20 through 25 show the dynamic response of the rear main gear, Strut 5. Figure 20 shows the tire deflection history. Maximum tire deflection does not occur on the first impact impulse, but on the second impulse which occurs after spoiler activation. Tire deflection

Contrails

AFFDL-TR-71-155

Part I

finally damps to approximately 0.22 ft to support its portion of the static weight of the aircraft. Figure 21 shows the ground force along the strut axis; once again, the maximum load, 350,000 lb, occurs after spoiler activation, and damps to where Strut 5 finally supports approximately 121,000 lbs of the aircraft static weight. Figure 22 shows strut velocity which finally damps to the expected zero value. Figure 23 shows strut displacement; the maximum displacement, 1.86 ft, occurs after spoiler activation and approaches the bottoming limit of 2.083 ft. Figure 24 shows the ground reaction moment about the wheel axle. The first large negative impulse is due to tire spin up. Controlled braking begins at 2.14 seconds; the braking moment to keep the tire at 0.2 coefficient of friction averages approximately 45,000 lb-ft. Figure 25 shows the tire angular rate history. The first negative impulse is due to tire spin up. The angular rate gradually reduces as the aircraft velocity slows to the taxi speed.

Figures 26 through 31 show the dynamic response of the forward main gear, Strut 3. Except for different impact time and magnitudes, Figures 26 through 31 are similar to Figures 20 through 25 for Strut 5. Figures 26 through 31 are presented primarily to emphasize the capability of the simulation to individualize each gear location.

Figures 32 through 44 show the dynamic response of the nose gear, Strut 1. More output on the nose gear is shown to indicate the general output capability that is available for each gear. Figure 32 shows the tire deflection for the nose gear. Tire deflection for this gear, 0.59 ft, is the largest of all the gears. This large deflection is due,

AFFDL-TR-71-155
Part I

predominantly, to a high impact velocity resulting from a nose down pitch rate caused by the main gear initial impact. Note that the impact was so severe as to cause the nose tire to bounce off the runway between 3.14 and 3.64 seconds. Computer output showed the bounce to be about 0.13 ft for this landing sequence.

Figure 33 shows the ground reaction along the nose strut. Except for the magnitude and bounce, this figure is similar to Figures 21 and 27 for struts 5 and 3, respectively. Figure 34 shows the resistance of the nose gear strut to movement. Figure 35 shows the upper chamber air pressure. Figure 36 shows the acceleration of the strut relative to the airframe. Figure 37 shows strut velocity. Figure 38 shows strut displacement. Figure 39 shows lower air chamber pressure and indicates that the secondary piston moved only once. Figure 40 shows the secondary piston acceleration relative to the main strut. Figure 41 shows the secondary piston velocity relative to the main strut. Figure 42 shows the secondary piston displacement. It may be puzzling that the lower chamber pressure in Figure 39 and the secondary piston displacement in Figure 42 do not return to their initial values; the reason is that in the integration logic near a physical constraint, the accuracy required was initially set by data input at 0.0208 ft. Figure 43 shows the wheel axle moment for the nose gear. Since no braking was done on the nose wheel, the axle moment is very small and nominally positive. Figure 44 shows the nose tire angular rate. During nose gear bounce, the tire angular rate remains at the value when the tire comes off the runway.

AFFDL-TR-71-155

Part I

4. TAKEOFF ROLL

As with the landing roll, capability in the takeoff roll is shown by computer plots. The planned takeoff roll was as follows: weight - 635,850 lbs; full flaps; command a 10-degree angle of attack at 100 ft/sec airspeed; and engines full throttle. Table II shows the list of major events that occur throughout this particular takeoff roll.

The aircraft was started at a near equilibrium position except for the engine pitch moments. Figure 45 shows the ground reaction pitch moment transmitted to the main airframe throughout the takeoff roll. The full throttle engine pitch moment is approximately 600,000 ft-lbs. The gear reaction to this nose up moment is damping to approximately -600,000 ft-lbs as the up elevator command is given at 12.40 seconds. Full up elevator is achieved at 13.40 seconds; this nose up moment also couples with the gear reaction and causes the ground reaction pitch moment to increase in the negative direction. As dynamic pressure increases, the up elevator causes the ground reaction pitch moment to become more negative until liftoff occurs at 33.40 seconds, at which time the ground reaction moment goes to zero.

Figures 46 and 47 show pitch rate and pitch angle, respectively. Figure 48 shows the ground reaction force transmitted to the main airframe normal to the longitudinal axis. The ground reaction begins at the aircraft weight, -635,850 lbs, and goes to zero as the airspeed increases and liftoff occurs. Figure 49 shows the sink rate history. Note the tendency of the aircraft to sink back onto the runway as the forward main gears and back main gears leave the runway. Figure 50 shows

TABLE II
TAKEOFF ROLL EVENTS

Time (Sec)	Event
0	Velocity 12.8 ft/sec
12.40	Velocity 100 ft/sec, begin up elevator
13.40	Full up elevator, 25°, achieved
25.20	Nose Strut 1 full extension
27.30	Nose tire 1 off runway
31.10	Struts 2 & 3 full extension
31.20	Tires 2 & 3 off runway
33.30	Struts 4 & 5 full extension
33.40	Airborne

the mass center altitude history, and Figure 51 shows the runway velocity build-up. Lift-off occurred at 33.40 seconds, 209.7 ft/sec airspeed, and 4170 feet of runway. Figures 52, 53, and 54 show the nose gear tire deflection, ground reaction, and strut displacement, respectively. Note the tendency of the engine and elevator pitch up moments to lessen nose gear loads. Nose tire liftoff occurred at 27.3 seconds. Figures 55, 56, and 57 show the same gear data for the forward main gear, Strut 3, which lifts off at 31.2 seconds. Figures 58, 59, and 60 show the same gear data for the rear main gear, Strut 5. Note that just prior to the aircraft becoming airborne, the loads in the rear main gear increase. This is not unexpected since the aircraft is pitching up and the back gears become the pivot point.

AFFDL-TR-71-155
Part I

SECTION IV

CONCLUSIONS

The concept of a single comprehensive, quantitative simulation of total system performance has yielded very promising results for the takeoff and landing problem. To date, use of the program's capability as a design tool to do tradeoff studies in major system component design has only just begun. In order to develop better technology, the Air Force Flight Dynamics Laboratory will continue to improve the TOLA simulation and use it as a tool to study the takeoff and landing problem.

AFFDL-TR-71-155

Part I

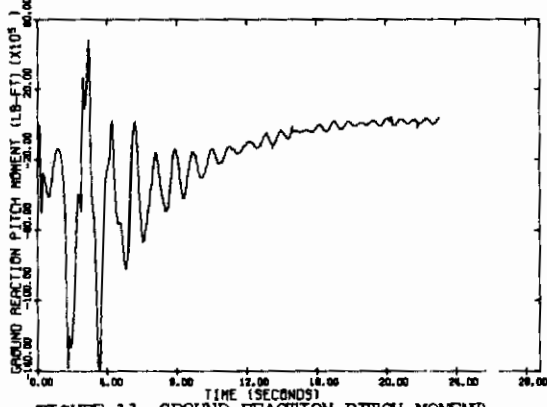


FIGURE 11 GROUND REACTION PITCH MOMENT

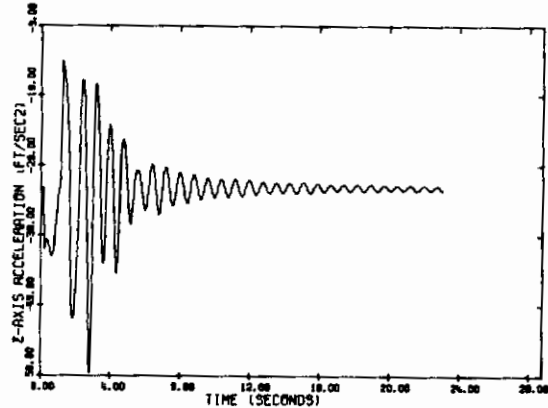


FIGURE 15 NORMAL AXIS ACCELERATION

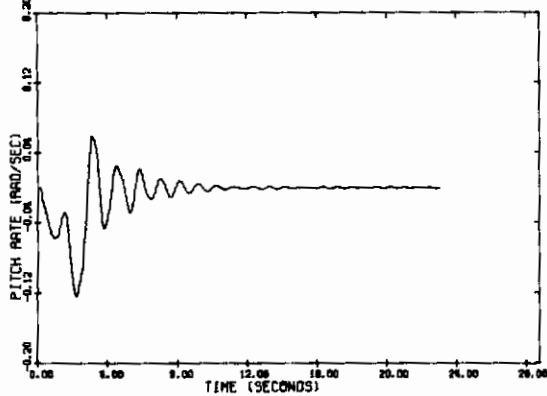


FIGURE 12 PITCH RATE

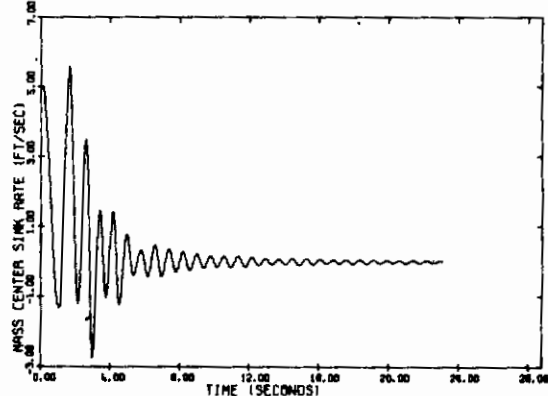


FIGURE 16 MASS CENTER SINK RATE

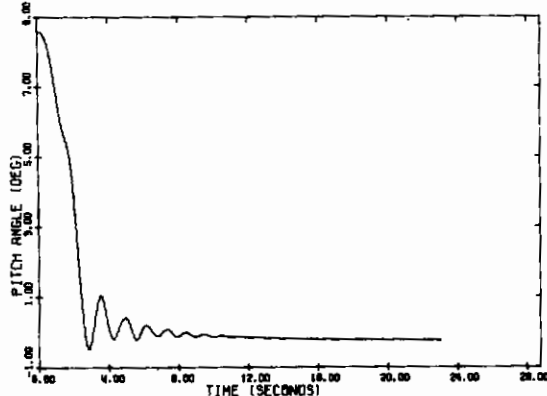


FIGURE 13 PITCH ANGLE

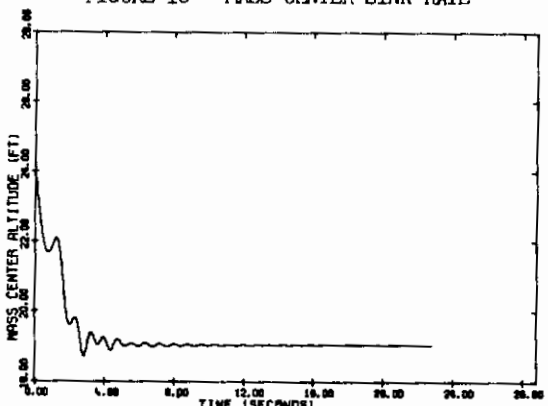


FIGURE 17 MASS CENTER ALTITUDE

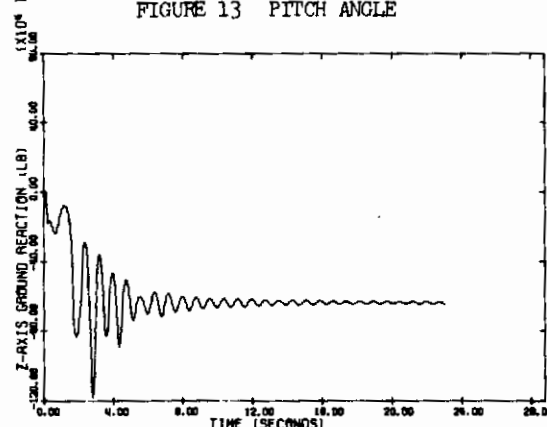


FIGURE 14 NORMAL AXIS GROUND REACTION

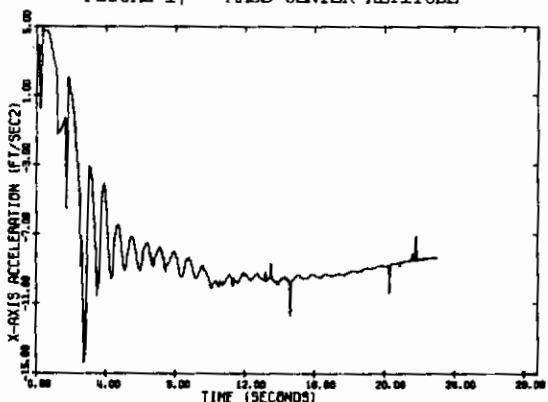


FIGURE 18 LONGITUDINAL AXIS ACCELERATION

AFFDL-TR-71-155

Part I

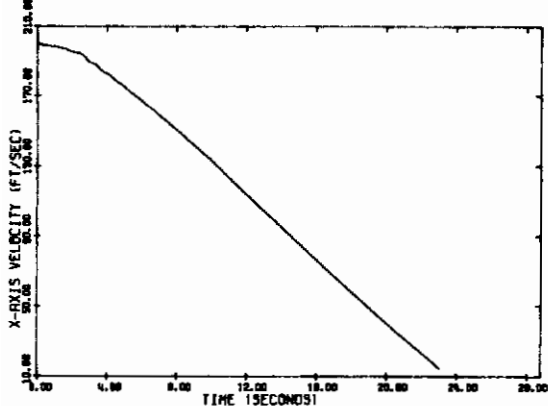


FIGURE 19 RUNWAY VELOCITY

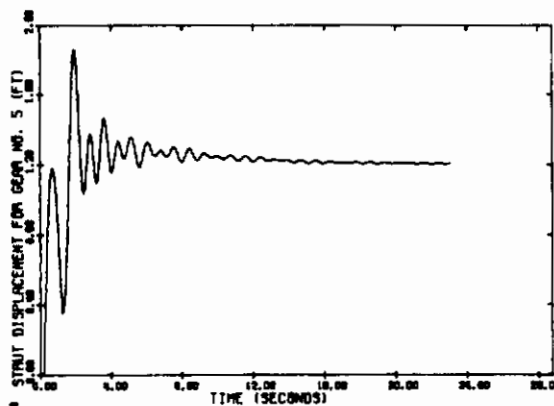


FIGURE 23 STRUT DISPLACEMENT GEAR 5

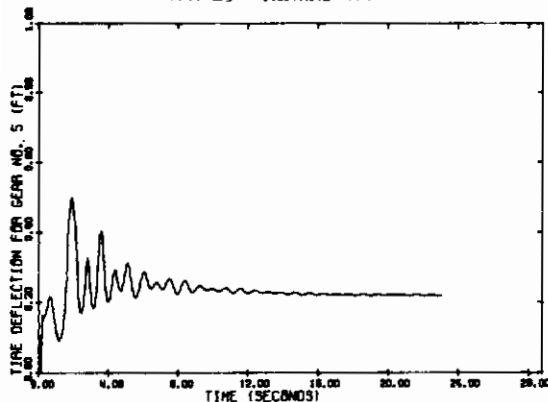


FIGURE 20 TIRE DEFLECTION GEAR 5

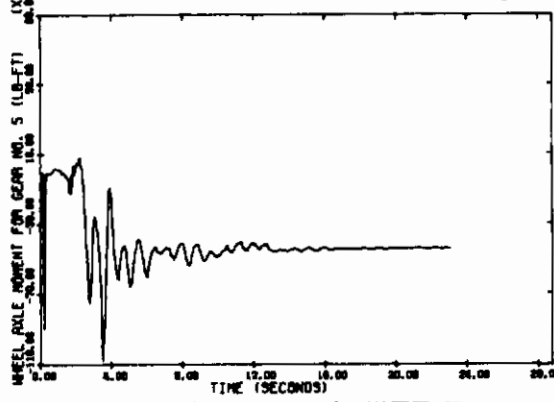


FIGURE 24 WHEEL AXLE MOMENT GEAR 5

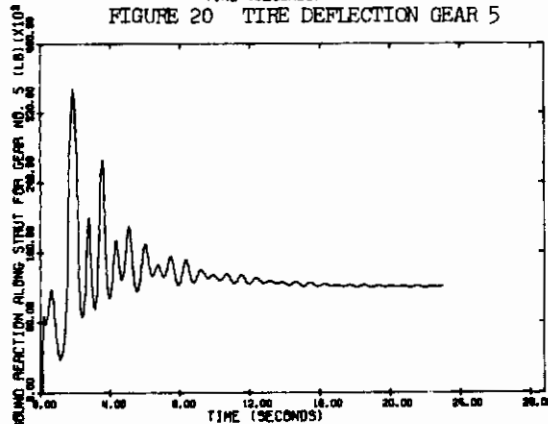


FIGURE 21 GROUND FORCE GEAR 5

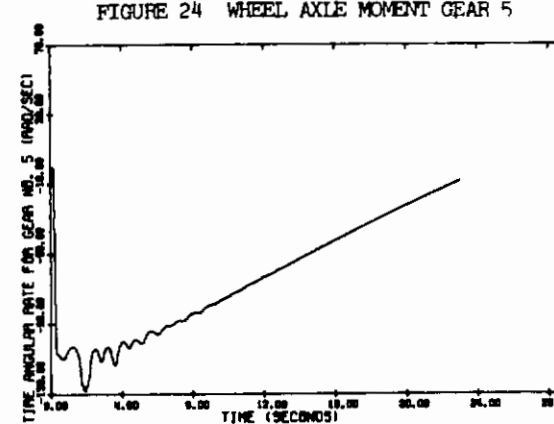


FIGURE 25 TIRE ANGULAR RATE GEAR 5

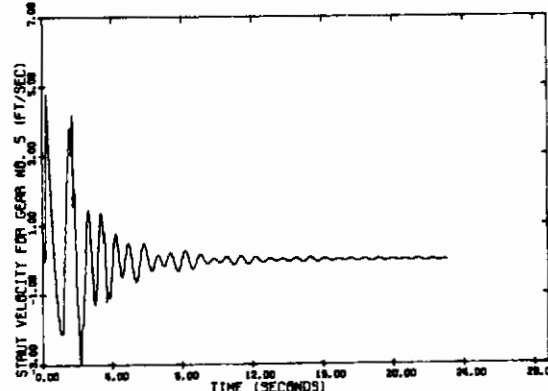


FIGURE 22 STRUT VELOCITY GEAR 5

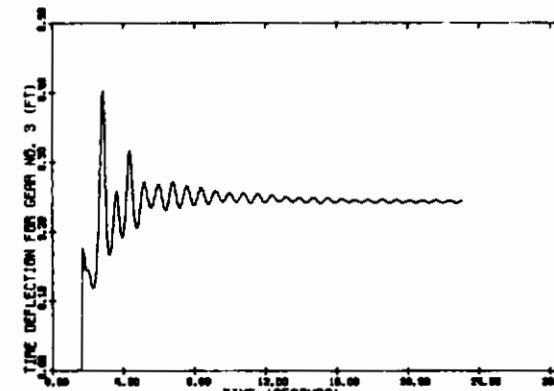
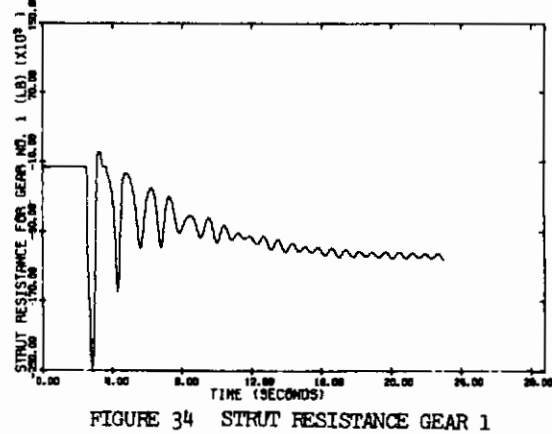
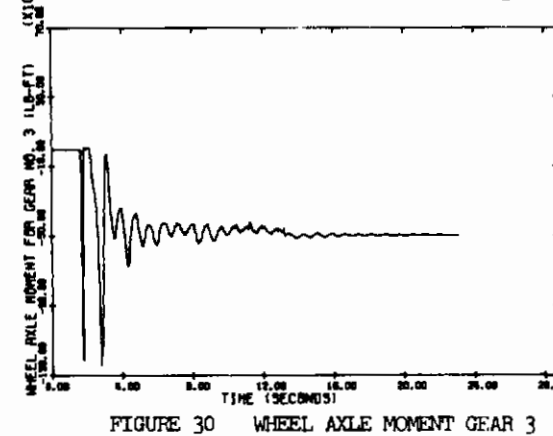
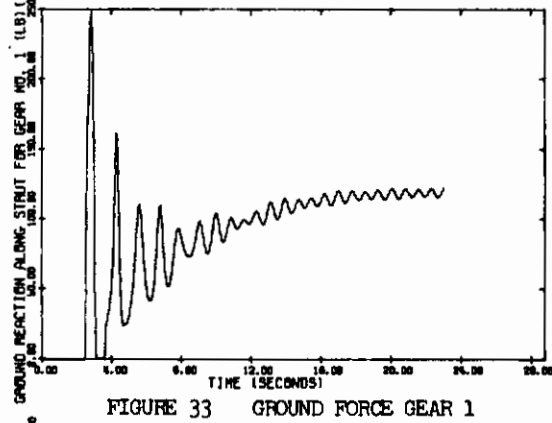
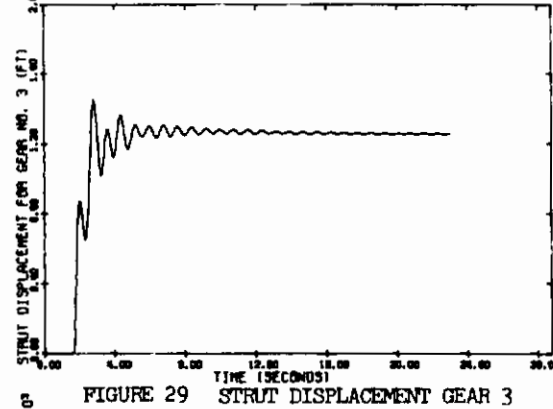
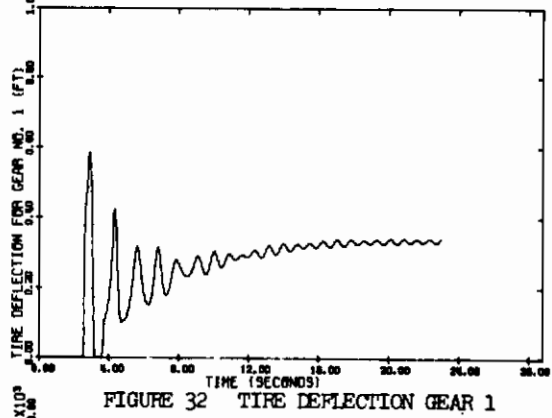
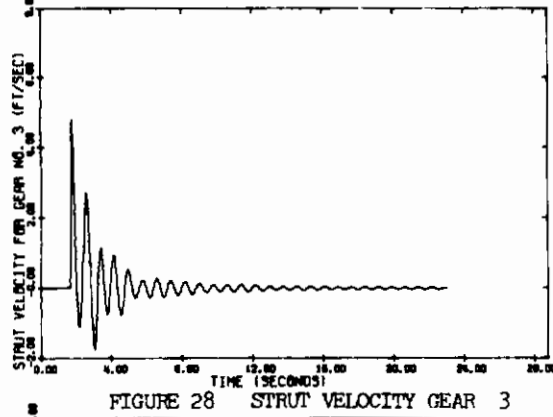
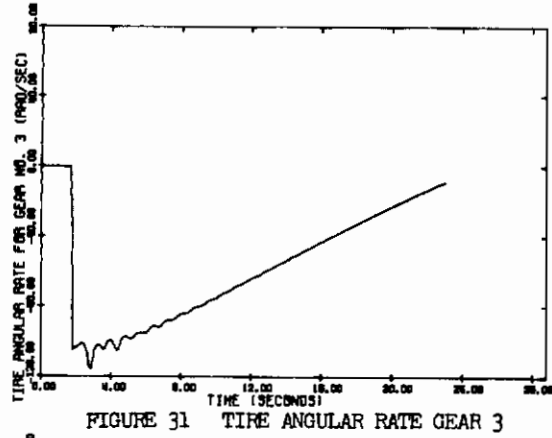
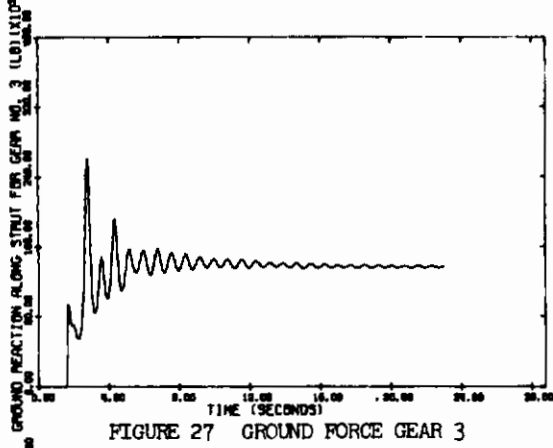


FIGURE 26 TIRE DEFLECTION GEAR 3

AFFDL-TR-71-155
Part I



AFFDL-TR-71-155
Part 1

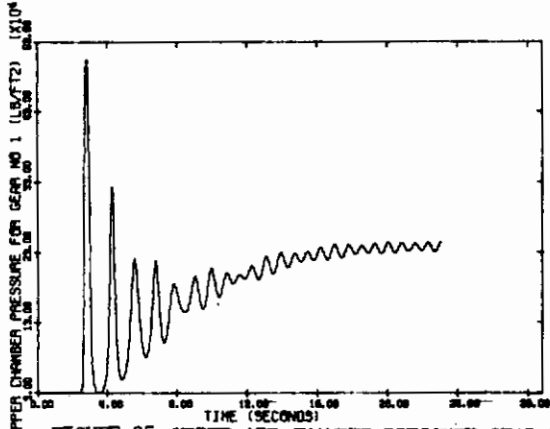


FIGURE 35 UPPER AIR CHAMBER PRESSURE GEAR 1

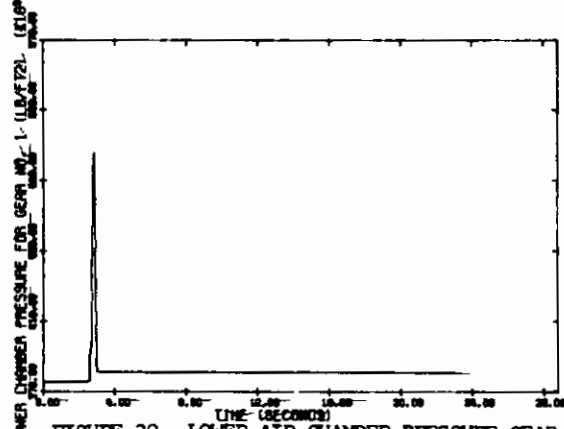


FIGURE 39 LOWER AIR CHAMBER PRESSURE GEAR 1

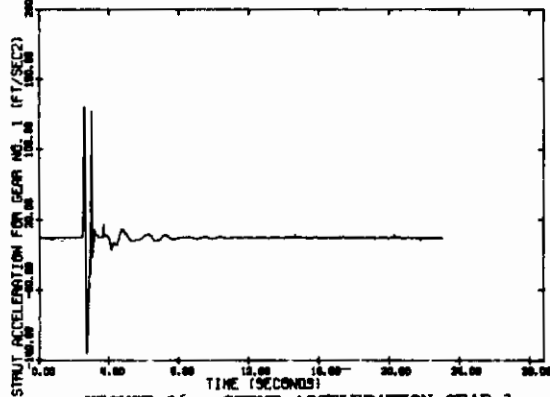


FIGURE 36 STRUT ACCELERATION GEAR 1

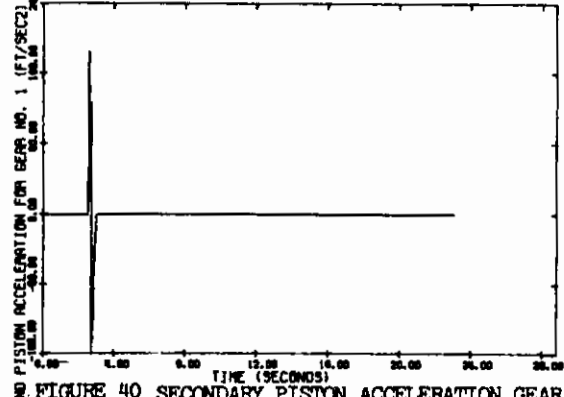


FIGURE 40 SECONDARY PISTON ACCELERATION GEAR 1

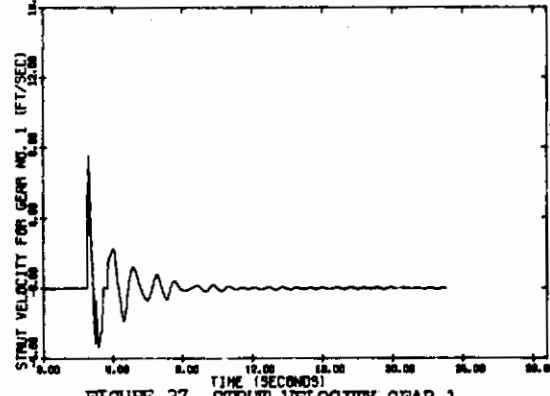


FIGURE 37 STRUT VELOCITY GEAR 1

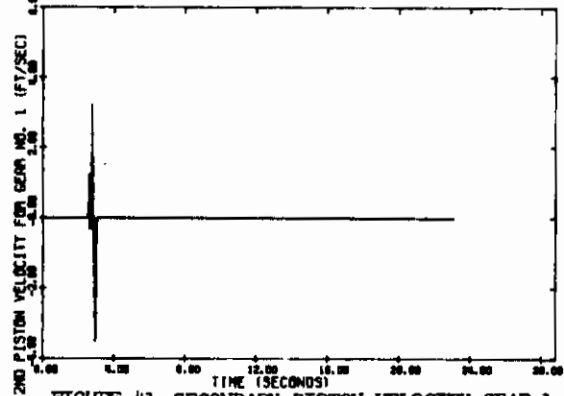


FIGURE 41 SECONDARY PISTON VELOCITY GEAR 1

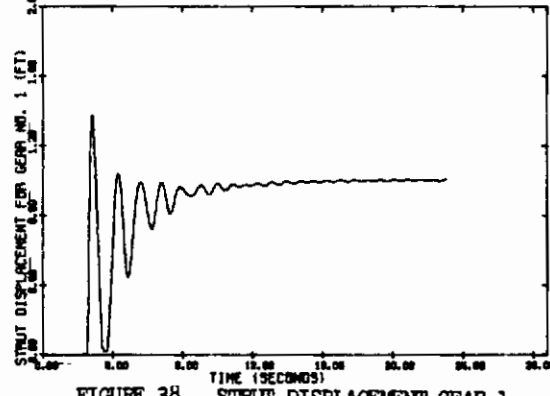


FIGURE 38 STRUT DISPLACEMENT GEAR 1

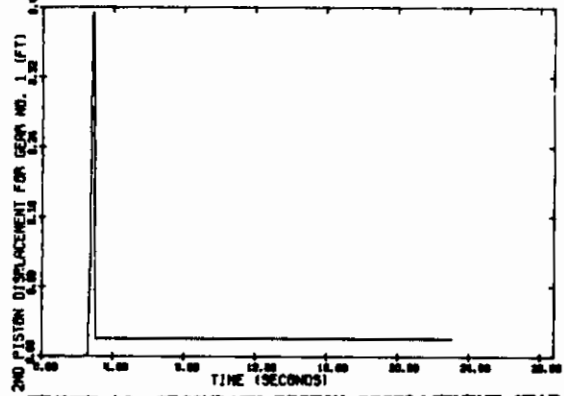


FIGURE 42 SECONDARY PISTON DISPLACEMENT GEAR 1

AFFDL-TR-71-155
Part I

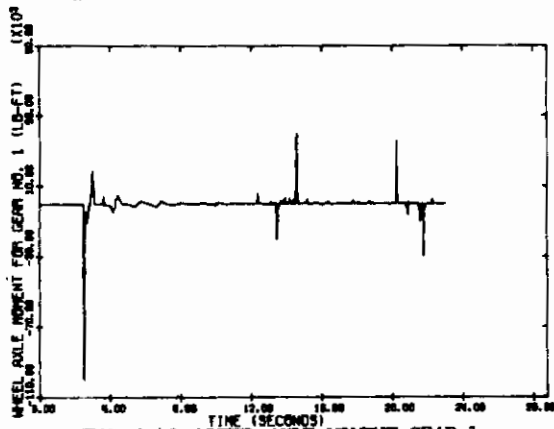


FIGURE 43 WHEEL AXLE MOMENT GEAR 1

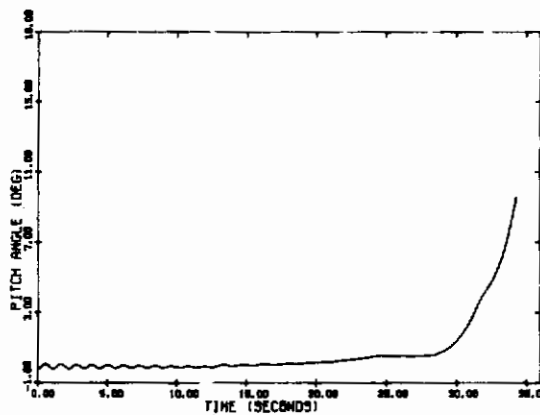


FIGURE 47 PITCH ANGLE

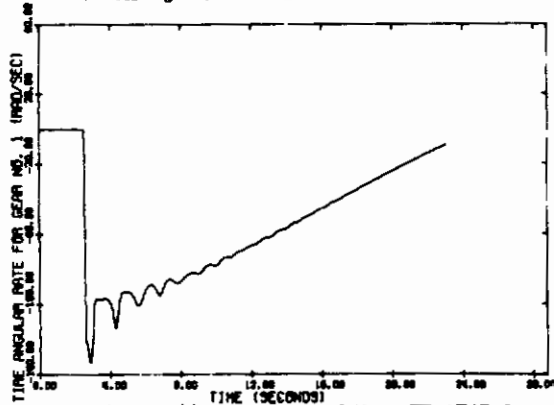


FIGURE 44 TIRE ANGULAR RATE GEAR 1

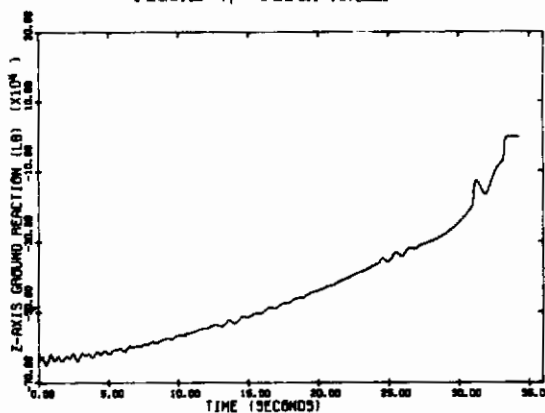


FIGURE 48 NORMAL AXIS GROUND REACTION

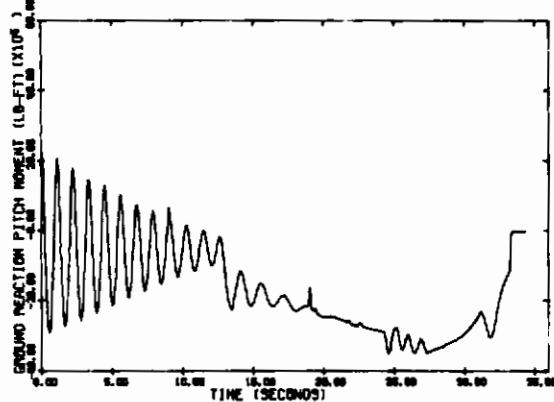


FIGURE 45 GROUND REACTION PITCH MOMENT

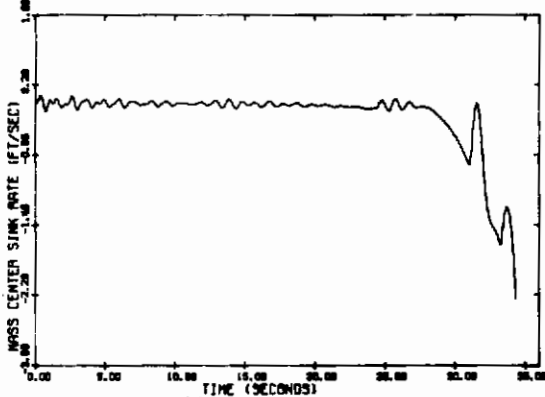


FIGURE 49 MASS CENTER SINK RATE

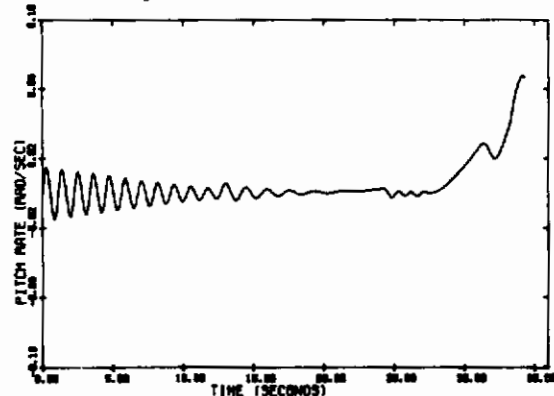


FIGURE 46 PITCH RATE

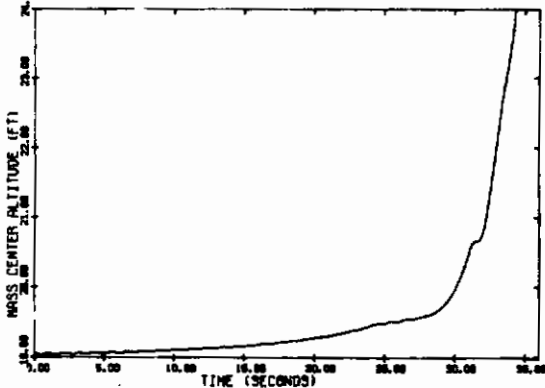


FIGURE 50 MASS CENTER ALTITUDE

AFFDL-TR-71-155
Part I

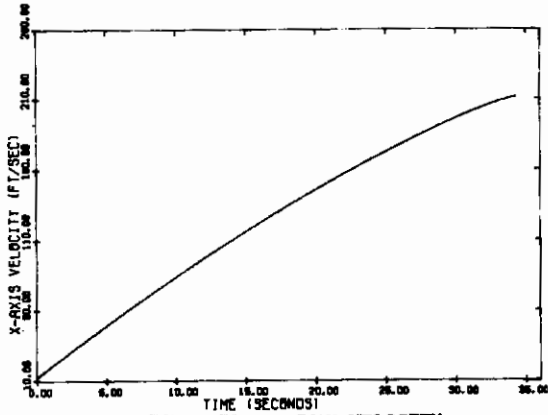


FIGURE 51 RUNWAY VELOCITY

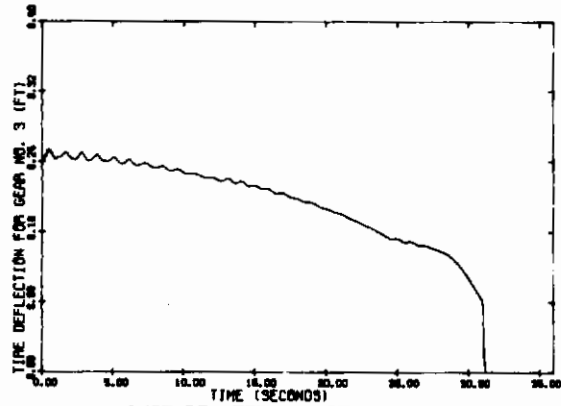


FIGURE 55 TIRE DEFLECTION GEAR 3

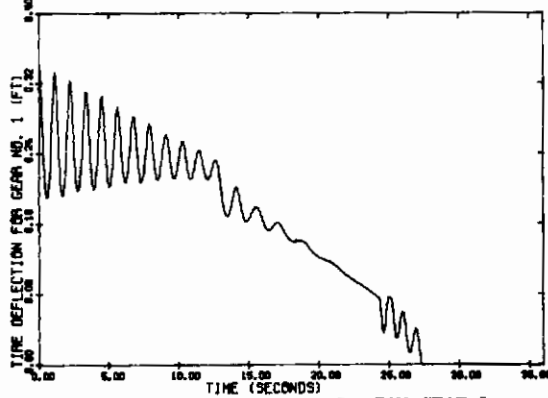


FIGURE 52 TIRE DEFLECTION GEAR 1

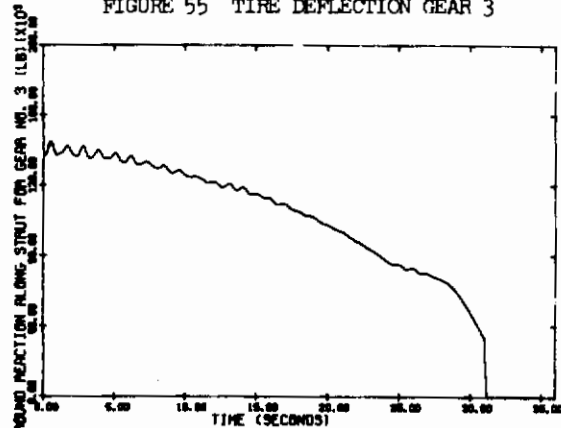


FIGURE 56 GROUND FORCE GEAR 3

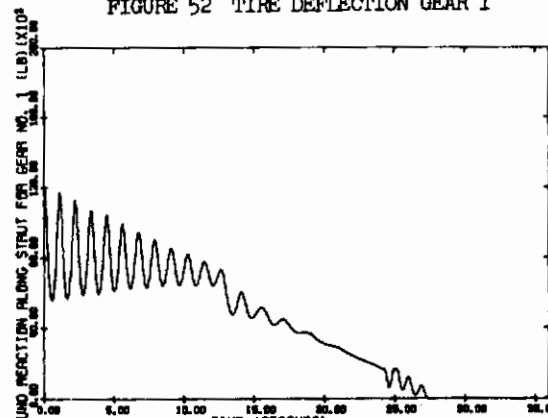


FIGURE 53 GROUND FORCE GEAR 1

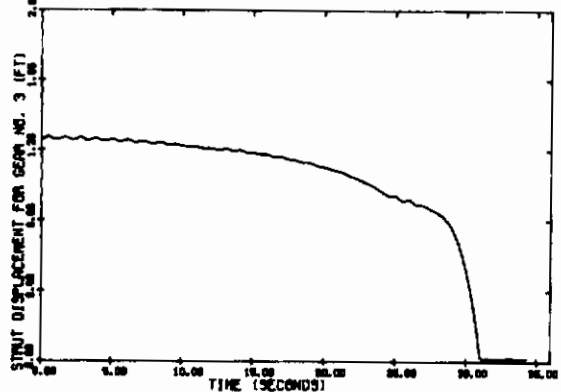


FIGURE 57 STRUT DISPLACEMENT GEAR 3

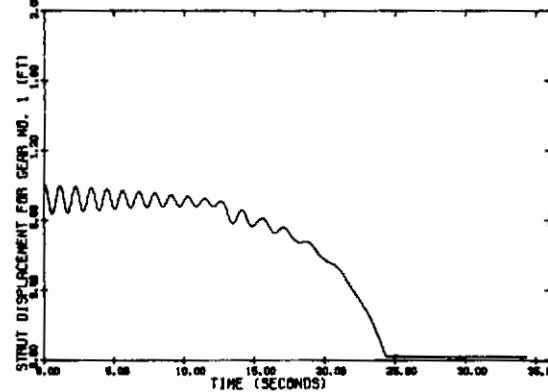


FIGURE 54 STRUT DISPLACEMENT GEAR 1

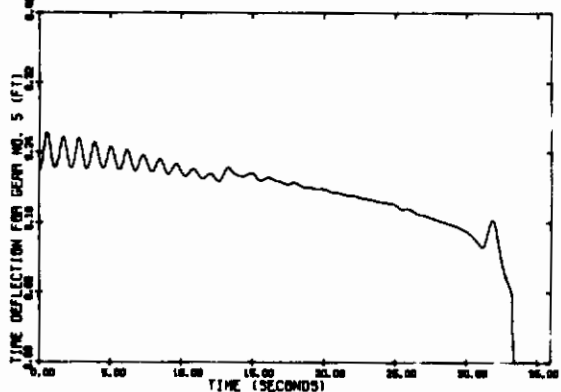


FIGURE 58 TIRE DEFLECTION GEAR 5

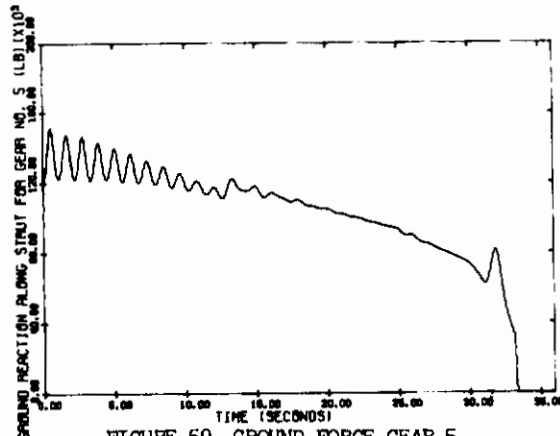


FIGURE 59 GROUND FORCE GEAR 5

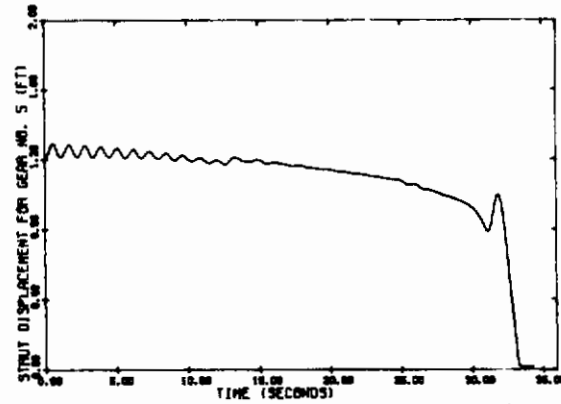


FIGURE 60 STRUT DISPLACEMENT GEAR 5

UNCLASSIFIED
Security Classification

DOCUMENT CONTROL DATA - R & D		
(Security classification of title, body of abstract and indexing annotation must be entered when the overall report is classified)		
1. ORIGINATING ACTIVITY (Corporate author) Air Force Flight Dynamics Laboratory Wright-Patterson Air Force Base, Ohio	2a. REPORT SECURITY CLASSIFICATION UNCLASSIFIED	
	2b. GROUP	
3. REPORT TITLE TAKEOFF AND LANDING ANALYSIS (TOLA) COMPUTER PROGRAM. PART I. CAPABILITIES OF THE TAKEOFF AND LANDING ANALYSIS COMPUTER PROGRAM		
4. DESCRIPTIVE NOTES (Type of report and inclusive dates)		
5. AUTHOR(S) (First name, middle initial, last name) Urban H. D. Lynch, Captain, USAF		
6. REPORT DATE February 1972	7a. TOTAL NO. OF PAGES 49	7b. NO. OF REFS
8a. CONTRACT OR GRANT NO.	9a. ORIGINATOR'S REPORT NUMBER(S) AFFDL-TR-71-155, PART I	
b. PROJECT NO. 1431	9b. OTHER REPORT NO(S) (Any other numbers that may be assigned this report)	
c. Task No. 143109		
d.		
10. DISTRIBUTION STATEMENT Approved for public release; distribution unlimited.		
11. SUPPLEMENTARY NOTES	12. SPONSORING MILITARY ACTIVITY Air Force Flight Dynamics Laboratory Air Force Systems Command Wright-Patterson Air Force Base, Ohio	
13. ABSTRACT TOLA is an acronym for a takeoff and landing analysis digital computer program. This part of the report discusses capabilities of the TOLA program. The program provides a complete simulation of the aircraft takeoff and landing problem. Effects simulated in the program include: (1) aircraft control and performance during glide slope, flare, landing roll, and takeoff roll, all under conditions of changing winds, engine failures, brake failures, control system failures, strut failures, runway length and control variable limits, and time lags; (2) landing gear loads and dynamics for aircraft with up to five gears; (3) multiple engine aircraft; (4) engine reversing; (5) drag chute and spoiler effects; (6) braking; (7) aerodynamic ground effect; (8) takeoff from aircraft carriers; and (9) inclined runways and runway perturbations. The program is modular so that glide slope, flare, landing, and takeoff can be studied separately or in combination. Results from this computer program compared well with those of other programs and actual test results. The program is very versatile through its completeness in simulation of the many systems and effects involved in the takeoff and landing problem. Application of TOLA has shown the need for a total system analysis since many unexpected results have been obtained.		

DD FORM 1473
1 NOV 65

UNCLASSIFIED
Security Classification

Contrails

Form 1473 Continued:

The TOLA program is ideal for dynamic tradeoff studies in aircraft design, landing gear design and landing techniques. The formulation is programmed for both the IBM 7094/7044 II Direct Couple Computer System in the FORTRAN IV Computer Language and the CDC 6400/6500/6600 Scope 3.3 Computer System in the FORTRAN EXTENDED Computer Language.

UNCLASSIFIED
Security Classification

14. KEY WORDS	LINK A		LINK B		LINK C	
	ROLE	WT	ROLE	WT	ROLE	WT
Takeoff and Landing Analysis						
Computer Program						
Glide Slope						
Flare						
Landing Roll						
Takeoff Roll						
Landing Gear Loads and Dynamics						
Vehicle Control						

Contrails